ARTICLES

Blue sunlight extinction and scattering by dust in the 60-km altitude atmospheric region

M. Ackerman, C. Lippens & C. Muller

Belgium Institute for Space Aeronomy, Circular Avenue 3, B-1180 Brussels, Belgium

P. Vrignault

Centre d'Essais des Landes, F-40520 Biscarosse, France

Twilight data obtained photographically from a stratospheric balloon platform in the autumns of 1980 and 1981 and in the spring of 1982 are presented for blue and red light. They indicate the presence of a light absorbing layer and of a scattering layer in the mesosphere at altitudes near 60 ± 10 km with a low scattering albedo (0.1) at 0.44 μm if it is accepted that both the extinction and scattering originate from dust. The optical efficiency of the layer increases more than 10 times when the wavelength of the interacting light changes from 0.65 to 0.44 μm. At the zenith and near sunset, the natural 0.44-μm extinction optical thickness and the cm^2 column scattering rate due to this layer are found to be 6.6×10^{-2} and 0.18 MR Å^{-1} respectively on 3 May 1982 above the south-west of France.

AEROSOLS have already been optically observed in the upper atmosphere from spacecrafts[1,2] and rockets[3–5]. Twilight observations[6,7] are also consistent with an upper-atmospheric particulate scattering. Other relevant experimental and theoretical work about upper atmospheric aerosols has been reviewed recently[8] in a study of their possible continuous and sporadic extraterrestrial sources and fate. On the other hand, it has been known for more than 40 years[9] that the atmosphere contains a source of optical extinction other than air and ozone in a supposedly transparent spectral region around 0.44 μm. This extinction has been observed day and night using stars and the Sun as light sources and has caused some concern to those[10–12] interested in the accurate determination of the extraterrestrial solar flux who have attributed the extraextinction to aerosols. It has more recently been attributed[13,14] entirely to NO_2 but the amount of this atmospheric constituent so deduced disagrees with observations based on the NO_2 extinction of IR radiation[15–17] and based on the differential extinction measurement of blue light[18–23]. Both the latter methods yield a smaller nitrogen dioxide abundance, 10–100 times less. Several authors[20,21,23] have indicated the presence of an unattributed absorption at 0.44 μm in the upper stratosphere.

Observation method

The observation method used here has been described previously[24] and leads to the determination for various scattering angles, θ, of the radiance of the sunlit atmosphere in units of solar radiance as given by

$$R_\theta / R_\odot = 6.79 \times 10^{-5} [Q_s n \sigma \phi_\theta / 4\pi) + n_M \sigma_\theta] \quad (1)$$

where Q_s, σ, ϕ_θ and n are the aerosol scattering efficiency, the geometrical cross-section, the phase function and the number of particles on the line of sight and where n_M and σ_θ are the number of air molecules on the line of sight and the differential air scattering cross-section[25].

Two improvements were implemented in the gondola. A neutral density filter identical to the one used to photograph the Sun at elevation angles larger than 5° was remotely moved in front of the cameras to photograph the solar image at zenith angles from 76° to 95° allowing to perform atmospheric absorption measurements. When the Sun was at elevation angles larger than 5°, the lower neutral density screens being removed from the cameras field of view, the gondola was rotated about its vertical axis by steps of 36° to obtain overlapping pictures of the Earth limb. The spectral bandwidths were 0.06 μm and 0.10 μm centred at 0.44 μm and 0.65 μm respectively.

The solar irradiance, I_0, is attenuated by the atmosphere leading to the measured irradiance

$$I = I_0 e^{-\tau} \quad (2)$$

where the optical thickness

$$\tau = \sum (\sigma_g n_g) + [(Q_s + Q_a) n \sigma] \quad (3)$$

where, σ_g and n_g are the extinction cross-sections of atmospheric gases and their numbers of molecules on the optical path whereas Q_a is the absorption efficiency of the aerosol. Q_s, n and σ have been defined in equation (1). The scattering albedo of the aerosol is

$$\omega = \frac{Q_s}{Q_s + Q_a} \quad (4)$$

and the extinction efficiency of the aerosol is

$$Q_e = Q_s + Q_a \quad (5)$$

Observations

The 1981 balloon flight took place from Aire sur l'Adour in the afternoon of 19 October. During the ascent in the stratosphere and at ceiling altitude, the winds carried the balloon mainly southwards in such a way that observations took place near 43 °N and 0°30′ W from 1530 to 1730 h GMT. Radar tracking was performed by the Centre d'Essais des Landes using a transponder carried with the gondola. Temperature and wind and ozone soundings were made, respectively starting at 1059 and 1336 h GMT from 44°21′N and 1°14′W. From the beginning of the scattering measurements to the end of the absorption measurements the balloon altitude decreased from 34.3 to 33.2 km.

The observed solar irradiances, I, at 0.44 μm are plotted against solar zenith angles, χ°, in Fig. 1*a* as well as their theoretically evaluated evolutions from $\chi = 91°$ towards smaller and larger values of χ. Rayleigh extinction by air has only been taken into account and represents fairly well the change of I from $\chi = 91°$ to 94.3°. A small maximum of excess extinction is observed centred at $\chi = 92.5°$. It corresponds to an optical thickness $\tau \cong 0.06$ which, if attributed to NO_2, leads to an integrated amount on the optical path of 10^{17} molecules cm^{-2}

0028–0836/82/350017—04$01.00

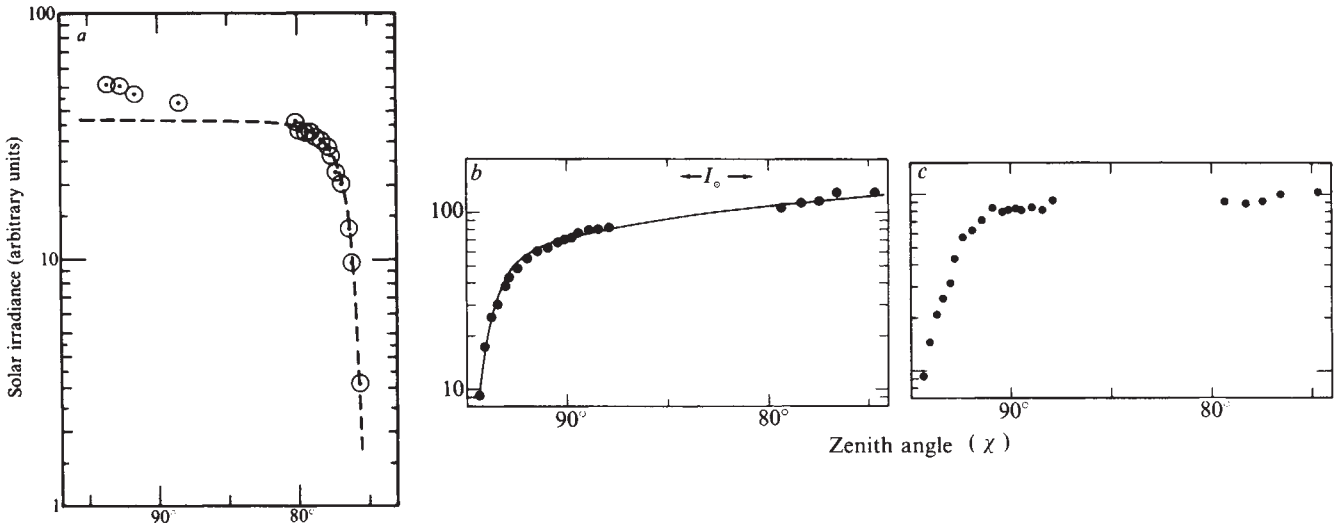

Fig. 1 *a*, Solar irradiances versus solar zenith angles observed on 19 October 1981. The circles represent the measurements while the dashed curve represents the expected variation from Rayleigh extinction, the main expected component at 0.44 μm. The observed solar irradiance at $\chi = 91°$ has been taken as a baseline for the computation. *b*, Solar irradiance observed on 3 May 1982 from a flight level of 6.1 mbar at 0.44 μm versus solar zenith angles χ. The values represented by the solid curve have been computed taking the extinction optical thicknesses shown in Fig. 2 and the extraterrestrial solar irradiance indicated by the arrows ($I_\odot$). *c*, As *a* but for 0.65 μm. The only absorber which can be considered in this case at $\chi = 90°$ is O_3 leading to a radiance reduction of 12%. No excess extinction can be detected with certainty.

at 28 km grazing altitude, a small value, if compared with previous determinations.

We wish to point out the difference between the theoretically expected and the observed evolution of I in the range $90° > \chi > 76°$. An excess of extinction decreasing slowly with increasing solar elevation is observed. This excess has been reported previously as shown in Table 1. Its slow evolution with zenith angle indicates that its cause lies well above flight altitude. No presently known gaseous absorber can explain the observed extinction. At 0.65 μm, an optical thickness change of 0.1 can be detected in the measurements from $\chi = 76°$ to 90° corresponding within experimental uncertainties to the expected variation of the ozone extinction. This leads to the first conclusion that a spectrally selective extinction takes place in the upper atmosphere at 0.44 μm, of which the origin is up to now unknown. Assuming that the Chapman function is valid for $\chi < 75°$, the total optical thickness at 0.44 μm on 19 October 1981 at $\chi = 90°$ and at 34 km altitude may approach unity.

On 3 May 1982, another evening flight took place from Aire sur l'Adour. The gondola reached a ceiling pressure level equal to 6.1 mbar with a maximum radar measured altitude of 36.6 km. The solar extinction data are shown in Fig. 1*b*. Here again an excess extinction appears at 0.44 μm for solar zenith angles <90°. Figure 1*c* shows the solar extinction curve at 0.65 μm. Taking into account an optical thickness of 0.1 in red light due to ozone at a zenith angle of 90°, no additional or excess absorption can be measured reliably.

The solid curve fitting the data on Fig. 1*b* is the result of a computation taking into account the optical thicknesses variation versus zenith angle shown in Fig. 2 for air (Rayleigh scattering), NO_2 and X, the unknown absorber.

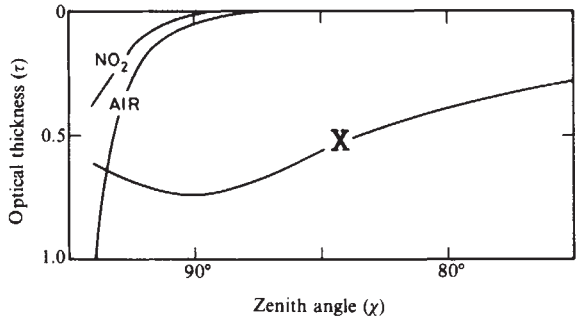

Fig. 2 Optical extinction thicknesses due to air, NO_2 and to the excess absorber, X, necessary to interpret the extinction observations of Fig. 1*b*.

To evaluate the effective altitude of X, the fraction of its maximum optical thickness τ, reached at $\chi = 90°$, has been computed for various values of χ. The result is shown in Fig. 3*a*. The relative value of the extraterrestrial solar radiance indicated in Fig. 1*b* has been chosen to provide the best fit to a theoretical dependence of τ versus χ leading to an effective altitude of 60 ± 10 km.

The NO_2 optical thickness shown in Fig. 2 associated with a molecular extinction cross-section of 6×10^{-19} cm^2 leads to a total stratospheric vertical content of NO_2 of 10^{16} molecules cm^{-2}.

The Earth limb radiances observed in the range of zenith angles, $\chi°$, from 86° to 93° are shown in Fig. 4 for two flights: 15 October 1981 at 37 km altitude (only mainly forward scattering is shown at 0.44 μm and at 0.65 μm) and 19 October 1981 at 34 km altitude (scattering angles from 14.5° to 166° at 0.44 μm and from 10.5° to 51° at 0.65 μm). The accuracy of the absolute values of $R_\theta/R_\odot$ are considered to be ±50% from one camera to the next, mostly due to the uncertainty in the evaluation of the high extinction of the neutral density screens. The accuracy of the relative values on a single camera is ±5%. The radiance variation observed compared with $\chi°$ on 15 October 1980 and shown here for $\theta = 13°$ is the best illustration

Table 1 List of extinctions in excess of Rayleigh scattering extinction observed at or near 0.44 μm and at solar zenith angles $\chi \cong 90°$ by means of instruments flown on various dates at various altitudes in the stratosphere

Date	Flight altitude (km)	Range of $\chi°$	Wavelength (nm)	$\Delta\tau$	Ref.
9 February 1977	40	75–80*	445	0.18	20
15 October 1980	38	81–84	440	0.28	This work[24]
19 October 1981	34.1	76–82	440	0.19	This work
19 October 1981	34.1	82–90	440	0.22	This work
June–July 1973	16.0	90°→	430	0.57	13

The changes of optical thickness, $\Delta\tau$, are indicated for various ranges of zenith angles. The observations made from Concorde in June–July 1973 lead to an absolute value of τ deduced from absolute solar irradiance data measured at 16 km altitude and at $\chi = 90°$ compared with extraterrestrial solar flux values.

* τ has deduced from a least square fit to the data available in this range of $\chi°$.

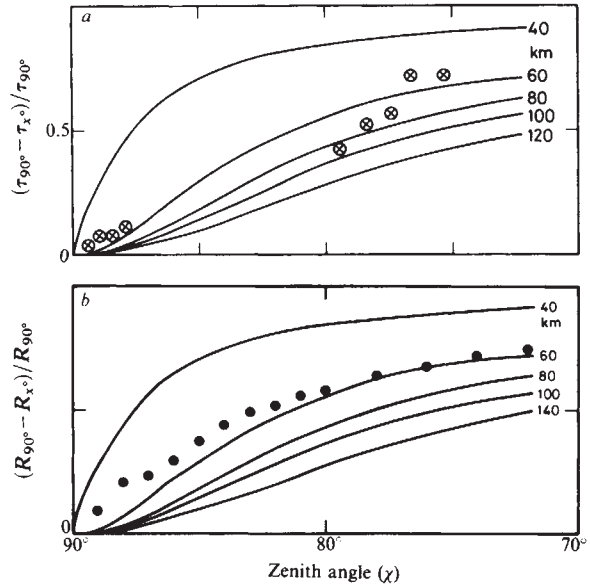

Fig. 3 *a*, Fraction of the excess extinction at $\chi = 90°$ plotted against zenith angles, χ. The computed variation of this quantity versus χ for various effective altitudes (40, 60, 80, 100 and 140 km) of the X absorber. *b*, As *a*, the fraction of the excess radiance observed at $\chi = 90°$ is plotted against χ. The expected variation of this quantity is also shown for various effective altitudes. It indicates an effective altitude of the excess radiance of nearly 60 km.

of the phenomenon that we wish to emphasize. Because at 0.44 μm, the Rayleigh scattering should dominate the scattering, a theoretical variation of the total number of air molecules on the line of sight versus χ is fitted to the observed radiance curve at $\chi = 90°$. At χ larger and smaller than 90° the observed radiance variation with χ is smaller than the theoretical one represented by the dotted curve. The cause of this difference is considered to be an excess of radiance originating from altitudes larger than the flight altitude. The dotted theoretical curve is shifted downwards to fit the observations at $\chi \cong 92.5°$ where the excess of radiance becomes small compared with the air Rayleigh radiance, because lower and lower altitudes are tangentially observed at progressively larger zenith angles where the increasing air density must eventually dominate the scattering dependence of zenith distance. It is also observed that the excess radiance decreases slowly above the horizontal line of sight when $\chi°$ becomes $< 90°$. The same phenomenon is observed on 19 October 1981 at 0.44 μm and at all scattering angles. In this case, however, the excess appears relatively smaller since the flight altitude was lower leading to a larger Rayleigh scattering due to air. A decrease of the blue and red colour ratio occurring near 1° solar depression angle, $\delta°$, has been observed in twilight studies[6] as well as an excess of blue light at $\delta = 0°$ which was attributed to multiple scattering. In the case of our observations, however, the air observed at $\chi \leqslant 90°$ is theoretically optically thin and multiple scattering does not explain the radiance excess, relative to pure air, linked with the anomalous radiance variation with zenith angle.

At 0.65 μm, a small excess of radiance in observed at $\theta = 20°$ on 15 October 1980. It is barely detectable at $\theta = 10.5°$ on 19 October 1981 and it cannot be detected at larger scattering angles, being probably too small relative to Rayleigh scattering at this low flight level.

For the 3 May, 1982 flight, one of the cameras was fitted with a blue filter-equipped wide angle lens ($f = 50$ mm) instead of the lens normally used ($f = 80$ mm). No neutral density screen was placed in front of this camera so that the sky could be viewed over a wider range of zenith angles. The calibration of this camera was performed by comparing film optical densities of identical features simultaneously photographed by means of another blue filter, neutral density screen equipped, camera.

The limb radiances observed at two flight levels, one during the balloon ascent and the other one at ceiling altitude, are plotted in Fig. 5 against zenith angles. The variations of the number of air molecules viewed on the optical path versus zenith angles are also represented and fitted to the observations at large zenith angles ($> 90°$) where pure air Rayleigh scattering must dominate.

As for the extinction in Fig. 3*a*, the fraction of the total excess radiance at $\chi = 90°$ has been plotted against zenith angles in Fig. 3*b*. Here again the measurements show an effective altitude for the excess radiance near 60 km. The radiance was also observed at 0.65 μm for two flight levels as it was done in Fig. 5 for 0.44 μm. The excess radiance determined in red light is 11 times smaller than in blue light. By spinning the gondola about its vertical axis by steps of 36°, the data necessary for

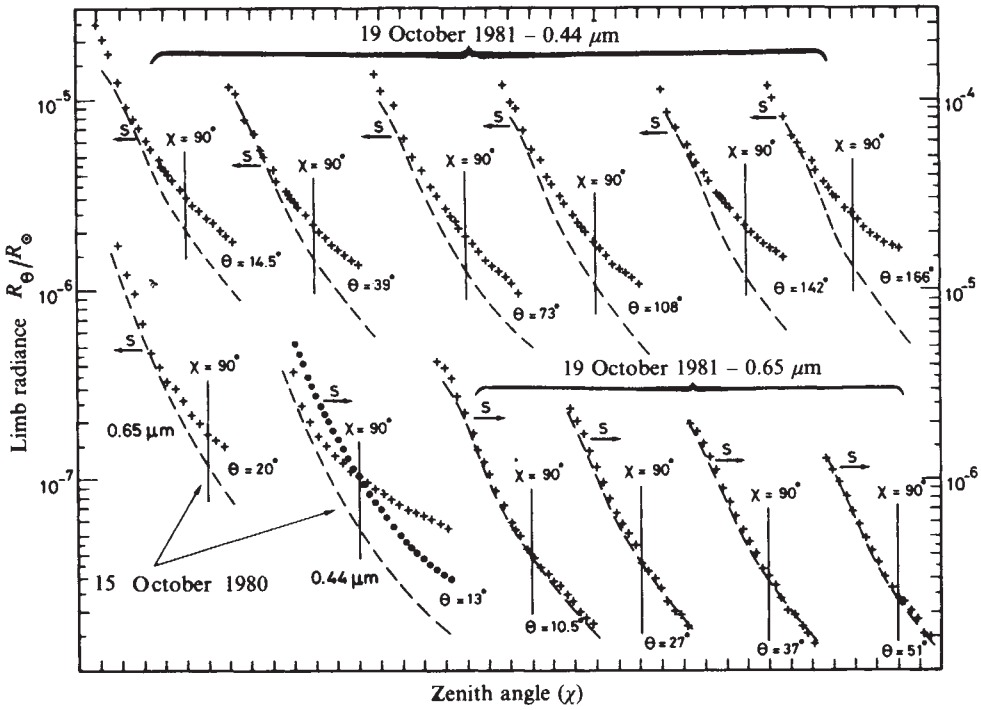

Fig. 4 Earth limb radiance $R_\theta/R_\odot$ in units of solar radiance observed on 15 October 1980, at 37 km altitude and on 19 October 1981 at 34 km altitude versus zenith angles $\chi°$. The observations are represented by crosses. The dashed and dotted (see text) curves represent total numbers of air molecules in arbitrary units which can be seen on the line of sight versus zenith angles $\chi°$. The arrows marked 's' indicate the ordinate scale relevant for each graph. The scattering angles $\theta°$, the wavelengths, 0.65 μm or 0.44 μm and the dates are also indicated. Average solar zenith angles were 78° on 19 October 1981 and 80° on 15 October 1980. For each case a vertical line indicates the $\chi = 90°$ position on the abcissa where an angular difference of 1° separates two ticks, zenith angles increase towards the left-hand side of the figure.

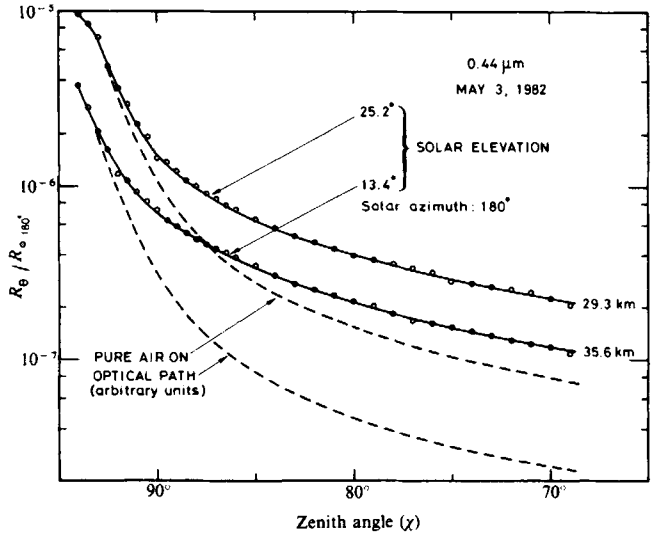

Fig. 5 Atmospheric radiance plotted against zenith angle at 0.44 μm from two flight levels on 3 May 1982. The pure air expected radiance is represented by the dashed curves.

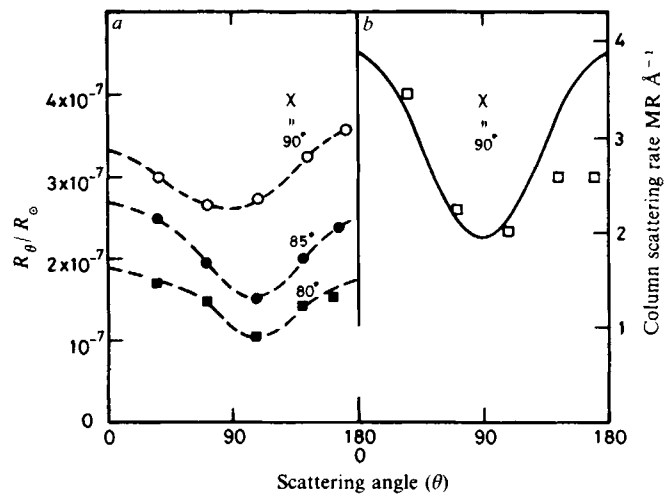

Fig. 6 Atmospheric excess radiance (*a*) observed at various zenith angles plotted against scattering angles $\theta°$. *b*, The pure air radiance phase function computed for the flight level (at 6.1 mbar) from the air differential cross-section[25]. Solar elevation is taken as 9° ± 1.5.

the determination of the phase function of the excess radiance have been obtained.

The phase functions are shown in Fig. 6 for three zenith angles in the case of the excess radiance. The values for air are those measured at $\chi = 90°$. However, in the latter case the angular variation reflects the phase function at zenith angles close to 93.5°, corresponding to grazing altitudes nearing 20 km. At these low altitudes the low stratospheric aerosols and perhaps the Earth sphericity induce illumination asymmetries when the solar azimuth changes from 36° to 180°. This most probably explains the deformation of the measured air phase function shown in Fig. 6 for air. At smaller zenith angles the air Rayleigh scattering becomes quickly very small compared with the excess radiance for which it becomes only a correction factor. The phase function observed at $\chi = 80°$ is for this reason used to deduce its characteristics.

The value of $Q_s n\sigma$ has been evaluated from these experimental data by means of the relationship

$$Q_s n\sigma = 1.85 \times 10^5 \sum_{0°}^{180°} (R_\theta / R_\odot)(\sin\theta \sin \Delta\theta/2) \qquad (6)$$

by zonal summation every 10° between 0° and 180°. The extinction due to scattering is found to be 2.6×10^{-2} which, according to Fig. 3*b*, leads, at $\chi = 90°$, to $Q_s n\sigma = 6.1 \times 10^{-2}$. On the other hand, the asymmetry parameter, $\langle \cos \alpha \rangle$, is found to be 0.06.

Discussion

The extinction and the excess of radiance have been shown to originate from an altitude near 60 km, in the mesosphere. They both also exhibit a large enhancement when the wavelength changes from 0.65 to 0.44 μm.

For an effective height of 60 km and an observation altitude of 35 km the optical depth factor increases 11.4 times from $\chi = 0°$ to 90°. The excess extinction observed leads, according to Fig. 3, to a zenithal optical depth of 6.6×10^{-2} of which 5.4×10^{-3} is due to scattering by the dust layer. If it is accepted that the dust is responsible for both extinction and scattering in the 60-km layer, the dust scattering albedo is 0.08. This low value is compatible with very small particles exhibiting an almost symmetrical scattering phase function. One way to explain the large scattering efficiency increase when the wavelength changes from 0.65 to 0.44 μm is to consider a colour-dependent complex index of refraction in this range with a non-negligible imaginary part of the index[26]. The dust would thus be made out of brownish matter. The complexity of the upper atmospheric dust probably having an extraterrestrial origin has already been pointed out[27].

Conclusion

The demonstration that a dust layer is present in the Earth's atmosphere at 60 km altitude would have a purely academic interest if it were not for its association with a non-negligible sunlight extinction and absorption *in situ* which makes it important for the Earth radiation balance, for the stratospheric and mesospheric photochemistry and energy budget and for the measurements of stratospheric trace species in blue light. These aspects justify the continued optical investigation of the layer from balloon gondola and from other platforms, and the use of other methods of investigation.

We thank the French Centre National d'Etudes Spatiales for the balloon operations and the Etablissement d'Etudes et de Recherches Météorologiques for atmospheric soundings.

Received 5 April; accepted 18 June 1982.

1. Giovane, F., Schuerman, D. W. & Greenberg, J. M. *J. geophys. Res.* **81,** 5388 (1976).
2. Kondratyev, K. Ja., Buznikov, A. A. & Pokrovsky, O. M. *Dokl. Akad. Nauk SSSR* **235,** 53–56 (1977).
3. Gray, C. R., Malchow, H. L., Merritt, D. C. & Var, R. E. *Spacecraft Rockets* **10,** No. 1 (1973).
4. Cunnold, D. M., Gray, C. R. & Merritt, D. C. *J. geophys. Res.* **78,** 920–931 (1973).
5. Rossler, F. *The Aerosol-Layer in the Stratosphere* (Deutsch-Französisches, St Louis, France, 1967).
6. Volz, F. & Goody, R. M. *J. atmos. Sci.* **19,** 385–406 (1962).
7. Meinel, M. P. & Meinel, A. B. *Science* **142,** 582–583 (1963).
8. Hunten, D. M., Turco, R. P. & Toon, O. B. *J. atmos. Sci.* **37,** 1342–1357 (1980).
9. Vassy, A. & E. *J. Phys.* **10,** 403–412 (1939).
10. Dunkelman, L. & Scolnik, R. J. *Opt. Soc. Am.* **49,** 356–367 (1959).
11. Labs, D. & Neckel, H. *Z. Astrophys.* **69,** 1–73 (1968).
12. Deluisi, J. J. *J. geophys. Res.* **80,** 345–354 (1975).
13. Blamont, J., Pommereau, J. P. & Souchon, G. *C.r. hebd. Séanc. Acad. Sci., Paris* **281,** 247–252 (1975).
14. Leroy, B., Hicks, E. & Vassy, A. *Ann. Geophys.* **36,** 205–208 (1980).
15. Ackerman, M. & Muller, C. *Nature* **240,** 300 (1972).
16. Ackerman, M. *et al. planet. Space Sci.* **23,** 651–660 (1975).
17. Coffey, M. T., Mankin, W. G. & Goldman, A. *J. geophys. Res.* **86,** 7331–7341 (1981).
18. Noxon, J. F. *Science* **189,** 547–549 (1975).
19. Kerr, J. B. & McElroy, C. T. *Atmosphere* **14,** 166–171 (1976).
20. Goldman, A., Fernald, F. G., Williams, W. J. & Murcray, D. G. *Geophys. Res. Lett.* **5,** 257–260 (1978).
21. Rigaud, P., Naudet, J. P. & Hugenin, D. *C.r. hebd. Séanc. Acad. Sci., Paris* **284,** 331–334 (1977).
22. Naudet, J. P., Rigaud, P. & Hugenin, D. *Geophys. Res. Lett.* **7,** 701–703 (1980).
23. Pommereau, J. P. thesis, Univ. Paris VI (1981).
24. Ackerman, M., Lippens, C. & Muller, C. *Nature* **292,** 587–591 (1981).
25. Penndorf, R. *J. opt. Soc. Am.* **47,** 176–183 (1957).
26. Kerker, M. *The Scattering of Light and Other Electromagnetic Radiation* (Academic, New York, 1969).
27. Bigg, E. K., Kviz, Z. & Thompson, W. J. *Tellus* **23,** 247–259 (1971).